MODELING DAMAGE OF CONCRETE CAUSED BY CORROSION OF STEEL REINFORCEMENT

JOŠKO OŽBOLT[*], FILIP ORŠANIĆ[*], MARIJA KUŠTER[†] AND GOJKO BALABANIĆ[±]

[*] Institute of Construction Materials, University of Stuttgart
Pfaffenwaldring 4, 70569 Stuttgart
e-mail: ozbolt@iwb.uni-stuttgart.de, www.iwb.uni-stuttgart.de

[†] Faculty of Civil Engineering, University of Zagreb
Kačićeva 26, 10000 Zagreb
marijak@grad.hr, www.grad.unizg.hr

[±] Faculty of Civil Engineering, University of Rijeka
Radmile Matejčić, br. 3, 51000 Rijeka
gojko@gradri.hr, www.gradri.uniri.hr

Keywords: Reinforced concrete, Corrosion, Damage, Chemo-hygro-thermo-mechanical model, Finite elements, Microplane model

Abstract: Reinforced concrete structures exposed to aggressive environmental conditions, such as structures close to the sea or highway bridges and garages exposed to de-icing salts, often exhibit damage due to corrosion. Damage is usually manifested in the form of cracking and spalling of concrete cover caused by expansion of corrosion products around reinforcement. The reparation of corroded structure is related with relatively high direct and indirect costs. Therefore, it is important to have a realible model, which is able to realistically predict influence of corrosion on the safety and durability of RC structures. In the present contribution a 3D chemo-hygro-thermo-mechanical model for concrete is presented. In the model the interaction between non-mechanical influences (distribution of temperature, humidity, oxygen, chloride and rust) and mechanical properties of concrete (damage), is accounted for. The mechanical part of the model is based on the microplane model. The application of the model is illustrated on two numerical examples in which transient 3D finite element analysis of RC specimens exposed to corrosion of steel reinforcement is carried out. In the first example the model is employed to investigate the pull-out capacity of corroded steel reinforcement from a concrete beam-end specimen, which was exposed to aggressive environmental conditions. Once the reinforcement is depassivated (begin of corrosion), corrosion rate is calculated and 1D corrosion contact elements are automatically activated generating radial compressive forces, which damage concrete cover. Finally, to predict the effect of corrosion on the pull-out capacity of reinforcement, the reinforcement bar is pulled out from the concrete specimen. The contact between reinforcement surface and concrete is simulated by the 1D discrete bond elements. The results of the computation are compared wit experimental data. In the second example the numerically predicted crack patterns due to corrosion of reinforcement in a beam are compared with experimental results. The influence of the anode-cathode position on the corrosion induced damage is investigated. The comparison between numerical results and experimental evidence shows that the model is able to realistically predict experimentally observed crack pattern and that the position of anode and cathode strongly influences the crack pattern and corrosion rate.

1 INTRODUCTION

Chloride-induced corrosion of steel bars in reinforced concrete has the main influence on the durabiliti of reinforced concrete (RC) structures [1]. It is well known that RC structures, which are exposed to aggressive environmental conditions, such as structures close to the sea or highway bridges and garages exposed to de-icing salts, very often exhibit damage due to corrosion [1,2]. This damage is usually manifested in the form of cracking and spalling of concrete cover, which is caused by the expansion of the corrosion products around the reinforcement bar. Repair of corroded concrete structures results in relatively high direct and indirect costs. Therefore, to predict durability of RC structures it is important to have a numerical tool, which is able to realistically simulate corrosion processes and the consequences for the structural safety.

The corrosion of reinforcement steel in aggressive environmental conditions is caused by a not sufficiently thick concrete cover or by its damage. Damage of the concrete cover can be caused by mechanical action (too high tensile stresses), or be a consequence of non-mechanical effects (temperature, shrinkage, etc.) or be induced by corrosion of reinforcement. The corroded cross-section of reinforcement bars has a smaller cross-section area and their bearing capacity is reduced. Moreover, with advanced corrosion, ductility of reinforcement, due to the pitting effect [3,4] and bond properties can be significantly reduced [2].

To estimate reduction of the cross-section area of reinforcement and to predict the increase of the volume of the corrosion product it is necessary to know the corrosion rate, i.e. corrosion current density in the corrosion unit. Furthermore, it is important to know how much of the corrosion product is transported into the concrete pores around the reinforcement bar and into the cracks that are distributed around the reinforcement bar. If more corrosion products are transported into the concrete pores and cracks, lower will be the pressure due to the expansion of the corrosion products.

Principally, the calculation of corrosion current density requires modeling of the following physical, electrochemical and mechanical processes: (1) transport of capillary water, oxygen and chloride through the concrete cover; (2) immobilization of chloride in the concrete; (3) transport of OH^- ions through electrolyte in concrete pores (4) cathodic and anodic polarization, (5) transport of corrosion products in concrete and cracks and (6) damage of concrete due to mechanical and non-mechanical actions (Bažant 1979). The importance of a three-dimensional (3D) numerical model, which can realistically simulate corrosion and its interaction with mechanical properties of concrete, is obvious. In the model the results of corrosion, such as the expansion of the corrosion products or the reduction of the cross-section of reinforcement, have an effect on the mechanical response of concrete structures. On the other hand, the mechanical properties, such as strength or fracture energy, also influence the corrosion process [1].

In a realistic computational model chemo-hygro-thermo processes must be coupled with mechanical processes, and the other way around. The theory for modelling of processes before and after depassivation of reinforcement in un-cracked concrete is well established, and presently there are a number of models available for simulation of these processes. This is well documented in the literature [1,5-10]. However, the response of structures made of quasi-brittle materials, such as concrete, subjected to mechanical or non-mechanical loading is characterized by cracking. In the last two decades significant progress in the modelling of such materials has been reached. Due to the complexity of concrete, computational modelling of damage processes is still a challenging task. This is especially true for the modelling of the influence of damage on transport processes in concrete. In the literature there are a very limited number of coupled 3D chemo-hygro-thermo mechanical models capable of realistic simulation of processes relevant for corrosion

reinforcement in cracked concrete [11,12]. Furthermore, there is no model that is able to simulate the transport of corrosion products through cracked concrete and its consequences for corrosion induced damage. The main difficulty in the formulation of such models is to quantify relevant parameters, which control processes before and after depassivation of reinforcement.

The present work gives an overview of the recently developed 3D chemo-hygro-thermo-mechanical model for concrete that is able to simulate complex non-mechanical and mechanical processes before and after depassivation of steel reinforcement [11,12]. The model was implemented into a 3D FE code and it was shown that it is able to realistically predict depassivation time of reinforcement as well as corrosion rate after depassivation of reinforcement. Furthermore, modelling of corrosion induced damage and transport of corrosion products through concrete pores and cracks is also discussed. The first part of the article gives a brief review over the theoretical background and implementation into the 3D FE code. In the second part the application of the model is illustrated on numerical examples in which transient 3D finite element analysis of RC specimens is carried out. The examples demonstrate the influence of the corrosion of reinforcement on damage of concrete. The results are compared with the available experimental results from the literature.

2 CHEMO-HYGRO-THERMO-MECHANICAL MODEL FOR CONCRETE

Steel in concrete is protected from corrosion by surface film of ferric oxide. The corrosion will start when the film is broken or depassivated. Depassivation can be caused by reaching a threshold concentration of chloride ions in concrete near steel surface [1]. According to current knowledge [5,13] corrosion of steel in concrete is an electrochemical process, which is controlled by electrical conductivity of concrete and steel surfaces, presence of electrolyte in the

concrete and the concentration of dissolved oxygen in the pore water near the reinforcement.

The calculation of corrosion current density and its consequence for concrete structures requires modelling of the above mentioned physical and electrochemical processes. In here presented 3D chemo-hygro-thermo-mechanical model these processes are coupled with the mechanical properties of concrete (damage).

2.1 Non-mechanical processes before depassivation of reinforcement

Transport of capillary water is described in terms of volume fraction of pore water in concrete by Richard's equation [14], based on the assumption that transport processes take place in aged concrete:

$$\frac{\partial \theta_w}{\partial t} = \nabla \cdot \left[D_w(\theta_w) \nabla \theta_w \right] \qquad (1)$$

where θ_w is volume fraction of pore water (m^3 of water / m^3 of concrete) and $D_w(\theta_w)$ is capillary water diffusion coefficient (m^2/s) described as a strongly non-linear function of moisture content [15]. Transport of chloride ions through a non-saturated concrete occurs as a result of convection, diffusion and physically and chemically binding by cement hydration product [14]:

$$\theta_w \frac{\partial C_c}{\partial t} = \nabla \cdot \left[\theta_w D_c(\theta_w, T) \nabla C_c \right] +$$

$$+ D_w(\theta_w) \nabla \theta_w \nabla C_c - \frac{\partial C_{cb}}{\partial t} \qquad (2a)$$

$$\frac{\partial C_{cb}}{\partial t} = k_r \left(\alpha C_c - C_{cb} \right) \qquad (2b)$$

where C_c is concentration of free chloride dissolved in pore water (kg_{Cl^-}/m^3 pore solution), $D_c(\theta_w, T)$ is the effective chloride diffusion coefficient (m^2/s) expressed as a function of water content θ_w and concrete temperature T, C_{cb} is content of bound chloride per mass of cement gel (g_{Cl^-}/kg_{gel}), k_r is binding rate coefficient, $\alpha = 0.70$ is constant [16].

Assuming that oxygen does not participate in any chemical reaction before depassivation of steel, transport of oxygen through concrete is considered as a convective diffusion problem [14]:

$$\theta_w \frac{\partial C_o}{\partial t} = \nabla \cdot \left[\theta_w D_o(\theta_w) \nabla C_o \right] + \\ + D_w(\theta_w) \nabla \theta_w \nabla C_o \qquad (3)$$

where C_o is oxygen concentration in pore solution (kg of oxygen / m^3 of pore solution) and $D_o(\theta_w)$ is the effective oxygen diffusion coefficient, dependent on concrete porosity p_{con} and water saturation of concrete S_w.

Based on the constitutive law for heat flow and conservation of energy, the equation which describes distribution of temperature (T) in continuum reads:

$$\lambda \Delta T + W(T) - c\rho \frac{\partial T}{\partial t} = 0 \qquad (4)$$

where λ is thermal conductivity (W/(m K)), c is heat capacity per unit mass of concrete (J/(K kg)), ρ is mass density of concrete (kg/m^3) and W is internal source of heating (W/m^3). More detail related to the strong and weak formulations of the processes up to the depassivation of reinforcement can be found in Ožbolt et al. [11].

2.2 Non-mechanical processes after depassivation of reinforcement

The active corrosion of steel will start when steel reinforcement is depassivated. The non-mechanical processes relevant for the propagation stage of steel corrosion in concrete are: (1) Mass sinks of oxygen at steel surface due to cathodic and anodic reaction, (2) The flow of electric current through pore solution and (3) The cathodic and anodic potential.

The oxygen consumption at the cathodic and anodic surfaces can be calculated as:

$$D_o(S_w, p_{con}) \frac{\partial C_o}{\partial n}\bigg|_{cathode} = -k_c i_c \, k_c \\ = 8.29 \times 10^{-8} \frac{\text{kg}}{\text{C}} \quad (5a)$$

$$D_o(S_w, p_{con}) \frac{\partial C_o}{\partial n}\bigg|_{anode} = -k_a i_a \, k_a \\ = 4.14 \times 10^{-8} \frac{\text{kg}}{\text{C}} \quad (5b)$$

where n is outward normal to the steel bar surface and i_c and i_a are cathodic and anodic current density (A/m2), respectively.

According to Butler–Volmer kinetics, in the present model kinetics of reaction at the cathodic and anodic surface can be estimated from :

$$i_c = i_{0c} \frac{C_o}{C_{ob}} e^{2.3(\Phi_{0c} - \Phi)/\beta_c} \quad i_a = i_{0a} e^{2.3(\Phi - \Phi_{0a})/\beta_a} \quad (6)$$

where C_{ob} is oxygen concentration at surface of concrete element exposed to seawater (kg/m^3), Φ is electric potential in pore solution near reinforcement surface (V), i_{0c} and i_{0a} are the exchange current density of the cathodic and anodic reaction (A/m^2), Φ_{0c} and Φ_{0a} are the cathodic and anodic equilibrium potential (V), β_c and β_a are the Tafel slope for cathodic and anodic reaction (V/dec), respectively.

The electric current through the electrolyte is a result of motion of charged particles and if the electrical neutrality of the system and the uniform ions concentration are assumed, can be written as:

$$\mathbf{i} = -\sigma(S_w, p_{con}) \nabla \Phi \qquad (7)$$

where σ is electrical conductivity of concrete. The equation of electrical charge conservation, if the electrical neutrality is accounted for and the electrical conductivity of concrete is assumed as uniformly distributed, reads:

$$\nabla^2 \Phi = 0 \qquad (8)$$

Rate of rust production J_r (kg/m^{2}s) and mass of hydrated red rust per unit length of rebar m_r (kg/m), respectively, are calculated as:

$$J_r = 5.536 \times 10^{-7} i_a \\ m_r = J_r \Delta t A_r \qquad (9)$$

where Δt is time interval in which the corrosion is taking place and A_r is the

corresponding surface of the steel reinforcement. In general, corrosion products have 2 to 7 times larger specific volume than corroded steel. Consequently, radial expansion forces around the reinforcement bar surface are generated, which can cause cracking of concrete.

From experiments [17] it is known that in the case of chloride type of corrosion the part of corrosion products penetrate into the pore of concrete around the reinforcement bar and relatively large amount of rust can be transported through radial cracks that are generated because of expansion of corrosion products. This transport is very much dependent on water saturation. As a consequence of the transport of rust there are two effects: (1) Rust and radial pressure over the anodic reinforcement surface are not uniformly distributed and (2) The mechanical effect of the corrosion products (damage of concrete) becomes less pronounced.

Mathematically speaking distribution of corrosion product (red rust) R (kg/m^3 of pore solution) into the pores of concrete and in the cracks is modelled as convective diffusion problem:

$$\theta_w \frac{\partial R}{\partial t} = \nabla \cdot \left[\theta_w D_r \nabla R \right] + D_w(\theta_w) \nabla \theta_w \nabla R \quad (10)$$

in which D_r is diffusion coefficient (m^2/s) of corrosion product. Note that Eq. (10) does not describe transport of red rust, however, it describes distribution of red rust which is produced in concrete (pores and cracks) as a consequence of the reaction of soluble species (that can dissolve in the concrete pore solution and subsequently migrate or diffuse through pores and cracks of concrete) with oxygen in pore water [17]. The penetration of soluble species into the pore close to reinforcement is modelled as a diffusion problem only. This is controlled by the first part of the right hand side of Eq. (10) assuming that diffusion coefficient D_r is independent of the water content. Furthermore, it is assumed that the penetration stops when a layer of concrete pores filled by rust reaches the thickness of 0.01 mm. Subsequent transport of soluble

species is possible only through the cracks that can be generated after the pores of concrete close to reinforcement are filled with corrosion products. Transport through cracks is modelled as convective diffusion problem.

It is important to note that at this stage of the model development the transport of rust is modelled only in a qualitative sense. The reason is the fact that there are no experimental results which can support the proposed model from the quantitative side. Therefore, in future the model prediction related to the transport of rust should be calibrated based on the systematic experimental investigations under realistic corrosion conditions. The problem is that such experiments are time consuming. Alternatively, evaluation of corresponding data from the literature needs to be carried out.

2.3 Chemo-hygro-thermo-mechanical coupling

The mechanical part of the model is based on the microplane model for concrete with relaxed kinematic constraint [18]. In the finite element analysis cracks are treated in a smeared way, i.e. smeared crack approach is employed. To assure the objectivity of the results with respect to the size of the finite elements, the crack band method is used [19].

The governing equation for the mechanical behaviour of a continuous body in the case of static loading condition reads:

$$\nabla \left[D_m \left(u, \theta_w, T \right) \nabla u \right] + \rho b = 0 \quad (11)$$

where D_m is material stiffness tensor, ρb is specific volume load and u is displacement field. In the mechanical part of the model the total strain tensor is decomposed into mechanical strain, thermal strain, hygro strain (swelling–shrinking) and strain due to expansion of corrosion product.

The inelastic strains due to the expansion of corrosion products are in the present formulation modelled by 1D corrosion contact finite elements. They are oriented in the radial direction and simulate the contact between reinforcement surface and surrounding concrete. The elements can take up only shear

forces in direction of reinforcement axes and compressive forces perpendicular to the surface of reinforcement. The inelastic radial expansion due to corrosion Δl_r is calculated as:

$$\Delta l_r = \frac{m_r}{A_r}\left(\frac{1}{\rho_r} - \frac{0.523}{\rho_s}\right) \tag{12}$$

where $\rho_r = 1.96 \times 10^3$ (kg/m^3) and $\rho_s = 7.89 \times 10^3$ (kg/m^3) are densities of rust and steel, respectively, 0.523 is the ratio between the mass of steel (m_s) and the corresponding mass of rust (m_r) over the unit length of reinforcement and A_r is the surface of corroded steel reinforcement bar that is represented with the corrosion contact element.

The stiffness of rust layer is assumed to be $E_r = 100$ MPa. In the model it is represented by the axial stiffness of the corrosion contact elements. To model bond between deformed steel reinforcement and concrete the shear resistance of the 1D contact element is defined by the discrete bond-slip relationship.

3 NUMERICAL IMPLEMENTATION

To solve the above discussed system of partial differential equations using finite elements, the strong form have to be rewritten into a weak form. The weak form of the system of the partial differential equations, which govern transport of capillary water and oxygen through concrete, chloride ingress into the concrete, binding of chloride by hardened cement paste, heat transport in concrete, distribution of electric potential, transport of corrosion products and equilibrium is carried out by employing the Galerkin weighted residual method [20]. The model is implemented into a 3D finite element code. The non-mechanical part of the problem is solved by using direct integration method of implicit type [20]. To solve the mechanical part, Newton-Rapshon iterative scheme is used. To avoid mesh size dependency as a regularization method simple crack band approach is employed [19]. Coupling between mechanical and non-mechanical part of the model is performed by continuous update of governing model parameters during the

incremental transient finite element analysis. For more detail see Ožbolt et al. [11,12].

4 NUMERICAL EXAMPLES

4.1 Bond resistance of corroded reinforcement - Beam-End specimen

In the first example the model is employed in the analysis of the beam-end specimen, which is often used to study bond resistance of reinforcement. Discussed are only results related to the processes after depassivation of reinforcement. Attention is devoted to damage of concrete caused by corrosion of reinforcement and its consequences on the pull-out capacity of deformed steel bar.

The investigated beam-end specimen with four bars placed in the corners is chosen according to the test method proposed by Chana [21] (Fig. 1). The specimen of the cross-section 200 x 200 mm^2 is used, which has shown to be the optimal choice. Namely, the optimization of the specimen geometry was focused on not to reach the yield strength of steel and to get such crack development for which all four bars of one specimen can be pulled out without disturbing each other. The horizontal support at the pull-out face of the specimen has a height of 100 mm whereas the vertical support is 90 mm wide and is placed at the rear top. The total embedment length of the reinforcement is 180 mm, diameter of the reinforcement is 12 mm and concrete cover is 20 mm. In the present numerical study only specimen without stirrups are investigated.
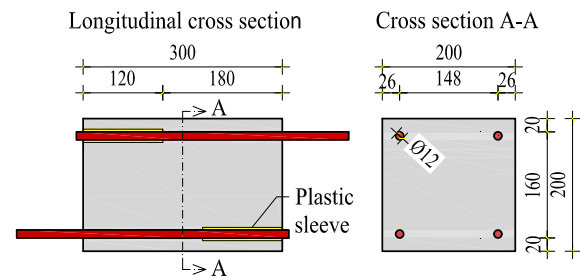

Figure 1: Cross sections of the specimen

Mechanical properties of concrete are taken as: Young's modulus $E_c = 29000$ MPa, Poisson's ratio $\nu_c = 0.18$, Tensile strength

f_t = 3.0 MPa, Uniaxial compressive strength f_c = 39 MPa and fracture energy G_F = 90 J/m^2. As mentioned before, mechanical model for concrete is based on the microplane model [18]. Reinforcement steel is assumed to be linear elastic with Young's modulus E_s = 200000 MPa and Poisson's ratio v_s = 0.33.
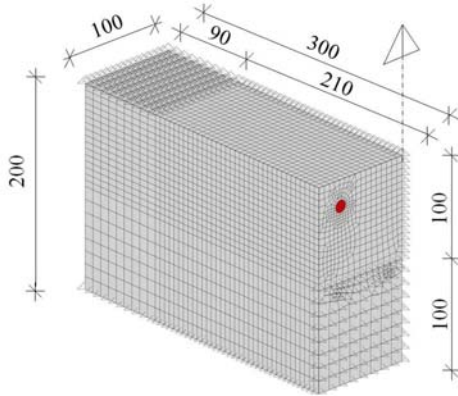

Figure 2: Model geometry (all in mm).

To study the influence of expansion of the corrosion products on damage of concrete cover and bond resistance, it is assumed that the anode along the reinforcement length is active (depassivated) at the start of the analysis. Therefore, only electric potential, current density and distribution of oxygen are calculated. To reduce computational time only 1/2 of the beam cross section is discretized by eight-node solid 3D finite elements (Fig. 2). It is assumed that along the reinforcement length embedded into concrete there are several anodic and cathodic regions (macro cells) with length and spacing of 24 mm. In each analyzed case the degree of water saturation is assumed to be constant over the entire volume of the specimen (S = 50%). Furthermore, it is assumed that the initial concentration of oxygen in the beam is 0.0085 kg of dissolved oxygen/m^3 of pore solution, which is also boundary condition at free surfaces of the beam. The dependence of the oxygen diffusivity and electrical conductivity on water saturation for good quality concrete (water-cement ratio w/c = 0.4) as well as other relevant parameters employed in the

computations of corrosion current density can be found in Ožbolt et al. [12]. For the transport of corrosion products through cracks, diffusivity coefficient is set to D_r = 2.2×10^{-16} m^2/s and the volume expansion factor of rust is assumed to be $\alpha_r = \rho_s/\rho_r$ = 4.0.

For the bond-slip constitutive law of contact corrosion elements the following parameters are used: total bond strength τ_b = 14.96 MPa, frictional strength τ_f = 5.90 MPa, and trashold slip values of: s_1 =0.85 mm, s_2 =1.65 mm and s_3 = 8.50 mm. The bond-slip relation is assumed to be independent of the corrosion rate. The length of discrete corrosion elements is set to l = 0.10 mm.
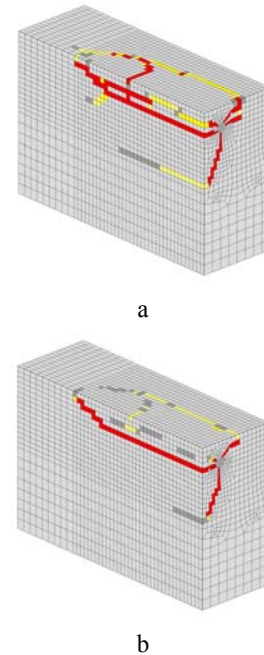

a

b

Figure 3: Crack patterns without (a) and with rust transport (b) 7 years after depassivation

The predicted damage (cracks) caused by corrosion of reinforcement after seven years, starting from the beginning of depassivation of steel, is shown in Figure 3. The crack patterns for the case without accounting for transport of rust through cracks are shown in Figure 3a and with the transport of rust in Figure 3b. As expected, with accounting for the transport of rust there is less damage. The first visible crack at the surface of the specimen (w = 0.05 mm) is observed after 200 and 350 days,

respectively. The maximal crack widths as a consequenece of corrosion are summarized in Table 1.

Similar crack patterns were observed in the experimental tests of Fischer [22], however, in the tests the corrosion was accelerated with the rate that is approximately 20 times higher than natural corrosion rate. Therefore development of corrosion induced damage in time cannot be directly compared with numerical prediction in which the natural corrosion conditions are assumed (aggressive, splash zone). Table 1 shows summary of predicted average and maximal thicknesses of the rust layer for the first specimen.

Tabel 1: Thickness of the rust and the maximum crack width (WOT - without and WT - with transport of rust)

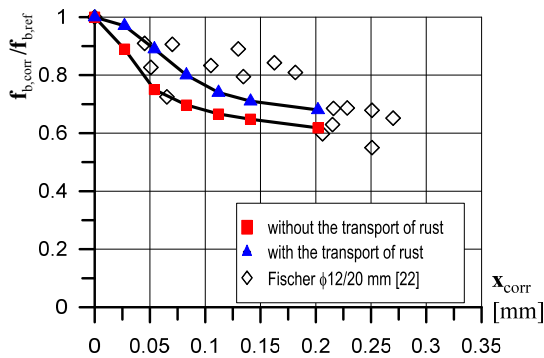| t	Rust thickness a [mm]				Max. crack width [mm]	
	WOT		WT		WOT	WT
	Aver.	Max.	Aver.	Max.		
1y	0.09	0.14	0.05	0.07	0.34	0.15
2y	0.20	0.33	0.10	0.17	0.76	0.39
3y	0.31	0.49	0.16	0.25	1.18	0.63
4y	0.41	0.66	0.21	0.33	1.55	0.89
5y	0.51	0.83	0.26	0.42	1.80	1.17
7y	0.72	1.16	0.37	0.59	2.30	1.49

Figure 4: Relation between loss of steel reinforcement due to corrosion in mm and pull-out capacity.

To study the influence of corrosion induced damage on the bond resistance, steel reinforcement bar is pulled out from the concrete specimen at t =0 (reference), 1, 2, 3,

4, 5 and 7 years, respectively. With the increase of corrosion rate the pull-out capacity decreases. The decrease is higher if no transport of corrosion products is assumed. The relative decrease of pull-out capacity is as a function of corrosion rate plotted in Figure 4. There is a nice agreement between experiments and calculations. It should be noted that numerical results with transport of rust should be actually compared with test data. Namely, in experiments [22] the significant transport of rust through cracks was observed, i.e. approximately 50% of generated rust was transported through cracks.

4.2 Influence of the anode-cathode positions on the corrosion induced damage

In the second example corrosion induced damage of reinforced concrete beam is computed assuming three different anodic-cathodic positions. The beam with three reinforcement bars is exposed to corrosion of reinforcement (see Fig. 5). In the analysis the segment of 130 mm is modeled. The mechanical properties of concrete are: modulus of elasticity of concrete E_c = 26200 MPa, modulus of elasticity of steel E_s = 200000 MPa, Poisson's ratio v = 0.18, tensile strength f_t = 1.92 MPa, uniaxial compressive strength f_c = 31.0 MPa and fracture energy G_F = 40 J/m^2. The same as in the previous example, only processes after depassivation of reinforcement are simulated. The analysis is performed for un-cracked good quality concrete (w/c = 0.4) assuming constant water saturations of 50%. In the analysis the same model parameters are used as in the previous example and they corresponds to severe splash conditions. Transport of rust through cracks is accounted for in the analysis, same as in the experiment [23]. However, it should be noted that in the experiment the beam was exposed to accelerated corrosion so that it is not possible to compare the corrosion related phenomena (corrosion rate, cracking, transport of rust, etc.) with respect to time.

One of still not solved problems when modeling corrosion of reinforcement is the fact that currently there is no algorithm, which can

predict the most critical combination between anodic and cathodic surfaces of reinforcement, i.e. that one which results to the highest corrosion. Therefore, to calculate corrosion rate it is in general case necessary to assume position of anode and cathode on the reinforcement surface. In order to investigate the influence of such assumption on the corrosion rate and corrosion induced damage, three different anode-cathode positions are considered: A, B and C (see Fig. 6). Case A represents the smallest and case C the largest portion of the reinforcement surface assumed to be anode. In the longitudinal direction distribution of anodic surfaces is taken the same for all three cases (see Fig. 5c).
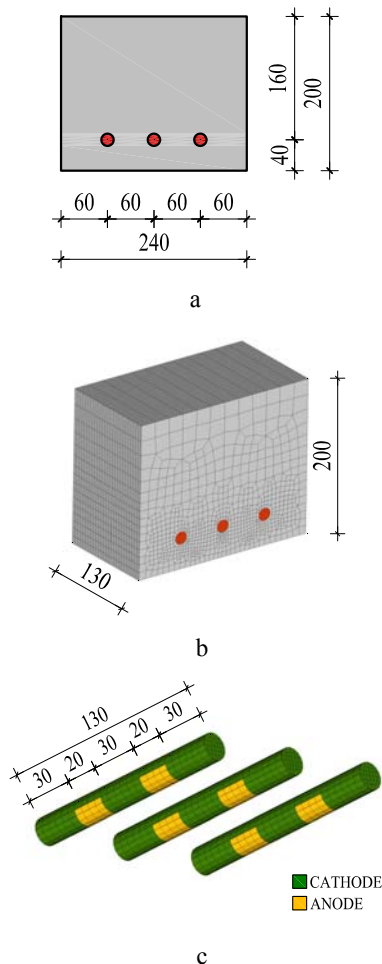
Figure 6: Anodic and cathodic part of the cross-section of the reinforcement

Figure 7 shows predicted crack patterns for the case B after 1.5, 3 and 6 years. The crack is plotted in terms of maximal principal strains. The red (dark) zone corresponds to the crack width of 0.10 mm. The first visible crack at the bottom beam surface (crack width $c_w = 0.05$ mm) is observed after 1.18 years for the case C. As expected, after 6 years of corrosion maximum crack width ($c_w = 0.58$ mm) is observed for the case C. Predicted crack patterns show that with increase of anodic surface the cracks which are close to the vertical beam surface tend to be more inclined. Furthermore, comparison of predicted crack patterns with the crack pattern observed in the experiment (see Fig. 8) shows that case B fits the best experimental crack pattern. This leads to the conclusion that in the experiment the anode-cathode position approximately corresponds to case B. From the evaluation of experimental results can also be seen that the most corroded part of the cross-section of the reinforcement bar was close to the bottom concrete surface of the beam.

Figure 5: (a) Beam cross section with 3 steel reinforcement bars, diameter $\phi = 16$ mm; (b) Finite element discretization; (c) Assumed distribution of the anodic and cathodic part over the surface of reinforcement
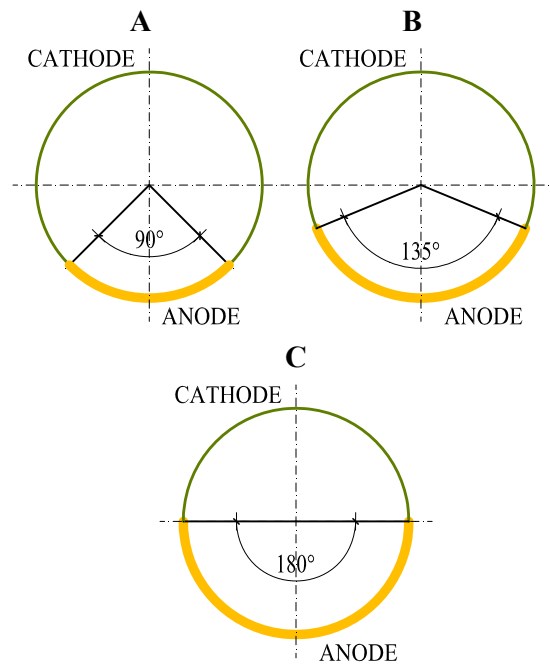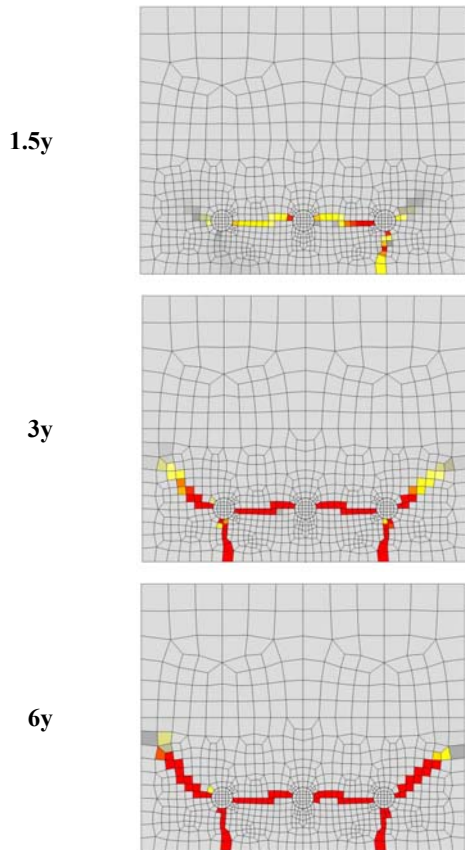
1.5y

3y

6y

Figure 7: Predicted corrosion induced crack patterns of the cross-section after 1.5, 3 and 6 years after depassivation for the case B

The numerical results (case B) show that the critical crack opening of 0.15 mm corresponds to the total rust production of 0.0091 kg/m of reinforcement bars. The critical crack forms 2.69 years after start of the corrosion process. This prediction is in good agreement with the statistical evaluation of measurements on structural elements under natural severe conditions [24].

a
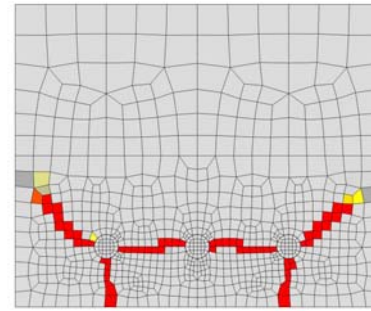
b

Figure 8: (a) Experimentaly observed [23] and (b) numerically predicted crack patterns of the cross-section, case B (t = 6 years)

5   SUMMARY AND CONCLUSIONS

The coupled 3D chemo-hygro-thermo-mechanical model for analysis of non-mechanical and mechanical processes related to the corrosion of steel reinforcement is presented. The application of the model is demonstrated on two examples. In the first case the study is performed on the beam-end specimen assuming aggressive environmental conditions (splash zone). The corrosion induced damage is predicted for different levels of corrosion. It is shown that already 1 year after depassivation of reinforcement there is cracking of concrete cover. Damage of concrete cover is less pronounced if the transport of rust through cracks is accounted for. Subsequently, to study the influence of the corrosion on the pull-out capacity of reinforcement, reinforcement bar is pulled out from the specimen for different corrosion levels. It is shown that the pull-out capacity after 7 years of corrosion is decreased by 37% and 43% for the case with and without transport of rust, respectively. The failure is due to the failure of concrete cover (splitting) and not to the pull-out of the bar from the concrete. Numerical results show very good agreement with experimental tests in which, for assumed environmental conditions, approximately 50 % of corrosion products were transported into cracks. As numerical analysis shows, this significantly reduces corrosion induced damage of concrete cover and contributes to higher pull-out capacity of corroded steel reinforcement.

The second example shows that the model is able to correctly predict crack pattern in the reinforced concrete beam exposed to severe conditions. Furthermore, it is shown how the choice of the anode-cathode position, which has to be assumed, influences the prediction of the crack pattern and corrosion of reinforcement. This important and complex aspect of the modeling of the corrosion of reinforcement is still not solved. Therefore, further development and calibration of the model is in progress.

6   REFERENCES

[1] Tuutti, K., 1993 *Corrosion of steel in concrete* , Technical report, Stockholm, (Swedish Cement and Concrete Research Institute)

[2] Cairns, J., 1998 *State of the art report on bond of corroded reinforcement*, Tech. Report No. CEB-TG-2/5, (CEB).

[3] Apostolopoulos, C.A. and Papadakis, V.G, 2008 Consequences of steel corrosion on the ductility properties of reinforcement bar, *Const. and Build. Mat.* 22, 2316-2324

[4] Cairns, J., Plizzari, G.A., Du, Y., Law, D.W. and Franzoni, C., 2005 Mechanical properties of corrosion-damaged reinforcement, *ACI Mat. Jour.* 102, 256-264

[5] Bažant, Z.P., 1979 Physical model for steel corrosion in concrete sea structures – theory, *Jour. of Struct. Div., ASCE* 105, 1137-1153

[6] Andrade, C., Diez, J.M. and Alonso, C., 1997 Mathematical modeling of a concrete surface "skin effect" on diffusion in chloride contaminated media, *Adv. Cement-Based Mat.* 6**,** 39-44

[7] Balabanić, G., Bićanić, N. and Đureković, A., 1996 The influence of w/c ratio, concrete cover thickness and degree of water saturation on the corrosion rate of reinforcing steel in concrete, *Cem. and Concr. Res.* 26, 761-769

[8] Balabanić, G., Bićanić, N. and Đureković, A., 1996 Mathematical modelling of electrochemical steel corrosion in concrete, *Journ. of Eng. Mech.* 122**,** 1113-1122

[9] Martín – Pérez, B., 1999 *Service life modelling of RC highway structures exposed to chlorides*, Dissertation, (University of Toronto)

[10] Glass, G.K. and Buenfeld, N.R., 2000 The infuence of chloride binding on the chloride induced corrosion risk in reinforced concrete, *Corr. Scien.* 42, 329-344

[11] Ožbolt, J., Balabanić, G., Periškić and G., Kušter, M., 2010 Modelling the effect of damage on transport processes in concrete, *Construction and Building Mat*erials 24,1638-1648

[12] Ožbolt, J., Balabanić, G. and Kušter, M., 2011 3D Numerical modelling of steel corrosion in concrete structures, *Corr. Scien.* 53, 4166-4177

[13] Glasstone, S., (1964): An introduction to electrochemical behaviour of steel in concrete, *Amer.-Concr. Insit. Jour.* 61, 177-188

[14] Bear. J and Bachmat, Y., 1991: *Introduction to modelling of transport phenomena in porous media*, (Kluwer Academic Publishers, Dordrecth)

[15] Leech, C., Lockington, D. and Dux, P., 2003 Unsaturated diffusivity functions for concrete derived from NMR images, *Mat. and Str.* 36, 413-418

[16] Saetta, A., Scotta, R. and Vitaliani, R., 1993 Analysis of chloride diffusion into partially saturated concrete, *ACI Mat. Jour.* **90** (5), 441-451

[17] Wong, H.S., Zhao Y.X., Karimi A.R., Buenfeld N.R. and Jin W.L., 2010 On the penetration of corrosion products from reinforcing steel into concrete due to chloride-induced corrosion, *Corr. Scien.* 52, 2469-2480

[18] Ožbolt, J., Li Y.-J. and Kožar I., 2001 Microplane model for concrete with relaxed kinematic constraint, *Int. Jour. of Solids and Struct.* 38, 2683-2711

[19] Bažant, Z.P.and Oh, B.H., 1983 Crack band theory for fracture of concrete, *RILEM* 93 155-177

[20] Belytschko. T, Liu, W.K. and Moran, B., 2001 *Nonlinear finite elements for continua and structures*, (New York, John Wiley & Sons Ltd)

[21] Chana, P.S., 1990 A test method to establish realistic bond stresses, *Mag. of Conc. Resear.* 42, 83-90

[22] Fischer C., 2012 *Beitrag zu den Auswirkungen der Bewehrungsstahlkorr. auf den Verbund zwischen Stahl und Beton*, PhD thesis, (University of Stuttgart, Institute of Construction Materials)

[23] Dong W., Murakami Y., Oshita H., Suzuki S. and Tsutsumi T., 2011 Influence of Bond Stirrup Spacing and Anchorage Performance on Residual Strength of Corroded RC Beams, *Journal of Adv. Concr. Tech.* 9: 261-275

[24] Thoft-Christensen P. 2000 Modelling of deterioration of reinforced concrete structures, *Proceedings of IFIP Conf. on Reliability and Optimization of Structural Systems*, Ann Arbor, Michigan, pp. 15-26